

# Ballistic limit velocity of tungsten alloy spherical fragment penetrating Ti/Al<sub>3</sub>Ti-laminated composite target plates

Yingbin Liu<sup>1</sup> , Chufan Yin<sup>1</sup>, Xiaoyan Hu<sup>1</sup> and Meini Yuan<sup>2</sup> 

## Abstract

To determine the ballistic limit velocity of titanium–titanium tri-aluminide (Ti/Al<sub>3</sub>Ti)-laminated composites under the action of tungsten alloy spherical fragments, a type of 12.7 mm ballistic gun loading system was used to test the tungsten alloy spherical fragments vertically impacting the Ti/Al<sub>3</sub>Ti-laminated composite targets with different thickness. The relationship between the ballistic limit velocity and the target area density of the Ti/Al<sub>3</sub>Ti-laminated composite was obtained. As the area density increased, the ballistic limit velocity and the ballistic energy absorbed by the target plate also enhanced. Based on the dimensional analysis and similarity theory, a simulation law of tungsten alloy spherical fragments penetrating Ti/Al<sub>3</sub>Ti-laminated composite targets with different thickness was studied and an empirical formula for the ballistic limit velocity was obtained. The research results had an important application value for the optimal design of the light armor protection structure.

## Keywords

laminated composites, ballistic limit velocity, tungsten alloy spherical fragment, penetration

## Introduction

With the continuous improvement of the penetration capability of ammunition weapons, some new protective materials have been developed and gradually replace the traditional homogeneous metal materials with the purpose of improving the protective performance.<sup>1</sup> Titanium–titanium tri-aluminide (Ti/Al<sub>3</sub>Ti)-laminated composite material has a promising application prospect in armor protection field because of its high specific strength, specific stiffness, and creep resistance of titanium tri-aluminide (Al<sub>3</sub>Ti) as well as good toughness of titanium (Ti).<sup>2</sup>

In the past 20 years, scholars had conducted a lot of studies on the preparation methods and mechanical properties of Ti/Al<sub>3</sub>Ti-laminated composites.<sup>3–15</sup> However, the research on the ballistic performance of Ti/Al<sub>3</sub>Ti-laminated composites are still relatively limited. Zelepugin and Zelepugin<sup>16</sup> used the finite element simulation and experimental method to study the failure processes of multilayer composites under dynamic loading, finding that the depth of penetration depended on the thicknesses of intermetallic and titanium alloy layers, where the composite target withstood the impact loading in the case of the mass ratio of nearly 4:1 (Al<sub>3</sub>Ti/Ti). Li et al.<sup>17</sup> established a compression

test model by a two-dimensional finite element method to analyze the evolution process of internal damage of Ti/Al<sub>3</sub>Ti-laminated composites under different loading strain rates. Grujicic<sup>18</sup> carried out a comprehensive computational engineering analysis to assess the suitability of the Ti/Al<sub>3</sub>Ti metal/intermetallic laminated composites (MILCs) used in both structural and add-on armor applications, and the results revealed that Ti/Al<sub>3</sub>Ti MILCs were more suitable for use in add-on ballistic than in structural armor applications. Cao et al.<sup>2</sup> used an explicit two-dimensional finite element

<sup>1</sup> School of Environment and Safety Engineering, North University of China, Taiyuan, China

<sup>2</sup> School of Mechatronic Engineering, North University of China, Taiyuan, China

Date received: 29 February 2020; accepted: 6 April 2020

### Corresponding authors:

Yingbin Liu, School of Environment and Safety Engineering, North University of China, Taiyuan 030051, China.

Email: ybliu@nuc.edu.cn

Meini Yuan, School of Mechatronic Engineering, North University of China, Taiyuan 030051, China.

Email: mnyuan@nuc.edu.cn



Creative Commons Non Commercial CC BY-NC: This article is distributed under the terms of the Creative Commons

Attribution-NonCommercial 4.0 License (<https://creativecommons.org/licenses/by-nc/4.0/>) which permits non-commercial use, reproduction and distribution of the work without further permission provided the original work is attributed as specified on the SAGE and Open Access pages (<https://us.sagepub.com/en-us/nam/open-access-at-sage>).

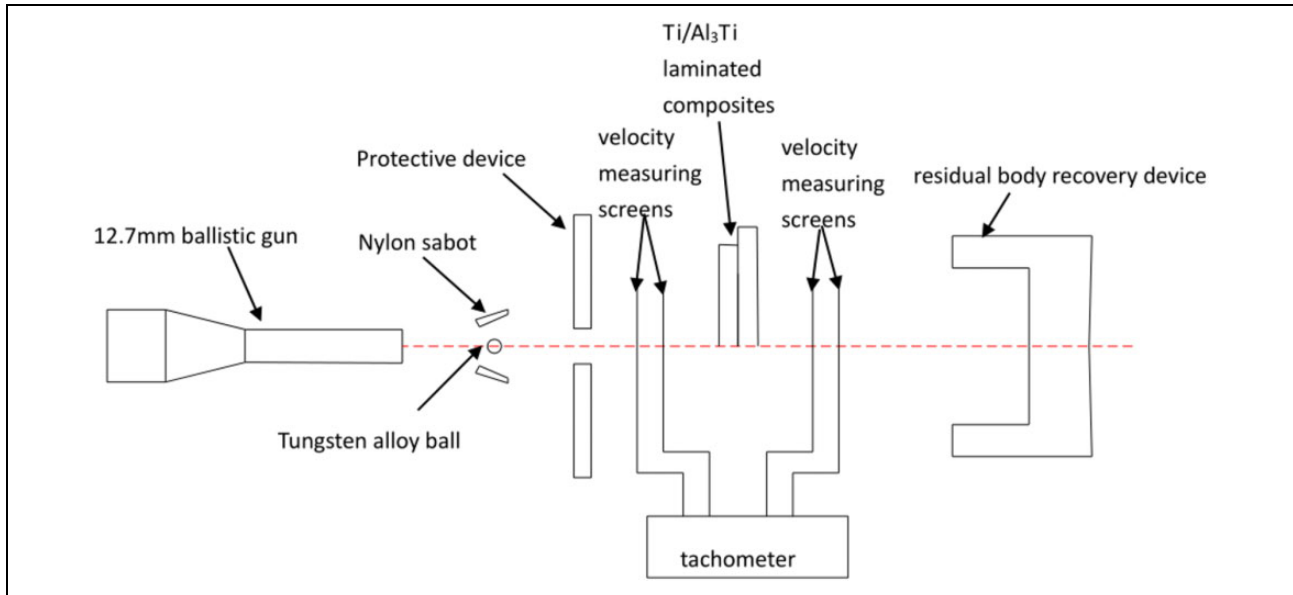


**Figure 1.** Sketch map of experimental design.

program of LS-DYNA software to study the ballistic performance and failure mechanism of Ti/Al<sub>3</sub>Ti under impact loading, then a finite element model of Ti/Al<sub>3</sub>Ti-laminated composite was established by considering the interface layer,<sup>19</sup> and then the damage degree of the matrix materials and the influence of the interface layer on the failure of the materials were analyzed.

Spherical fragments of tungsten alloy have advantages of simplest geometry, high density, strong holding velocity, and strong armor-piercing ability, which are widely used in prefabricated fragmentation warheads. For this reason, this article conducted an experimental study on the ballistic limit velocity of tungsten alloy spherical fragments vertically penetrating Ti/Al<sub>3</sub>Ti-laminated composites with different thickness and proposed an empirical relationship of ballistic limit velocity with dimensional analysis. The research results had an important application value for the optimal designs of the fragmented warhead and the light armor protection structure.

## Experimental

The penetration body was a tungsten alloy spherical fragment with a diameter of 9.45 mm and a mass of 8.1 g. Ti/Al<sub>3</sub>Ti-laminated composites were prepared by the endothermic semisolid reaction and self-propagating synthesis, and the preparation process was described in our previous work.<sup>15</sup> The ballistic experimental device and the arrangement are shown in Figure 1, which included a fragment-specific launcher, a protective device, a fragment velocity test system, a target rack, and a residual body recovery device. The fragmentary launcher was a 12.7 mm ballistic gun, and the velocity was controlled by the amount of gunpowder. To ensure the tightness required for the launch and

to achieve the specified velocity, the tungsten alloy ball was placed in a concave nylon sabot. After the sabot flew away from the muzzle, the tungsten alloy ball was separated from the sabot under the action of air resistance. The sabot was also broken for the impact. The broken sabot fragments could be intercepted by the protective plate, and the ball would fly to the target plate through the small hole in the center of the protective plate. The velocities of the residual body and the ball hitting the target were completed by a couple of velocity measuring screens before and after the target and a tachometer, respectively. When the impact velocity was higher than the ballistic limit velocity, its residual body and plug as well as the chipped debris on the back of the target would be collected by the residual body recovery device after the ball penetrates the target plate.

## Results and discussion

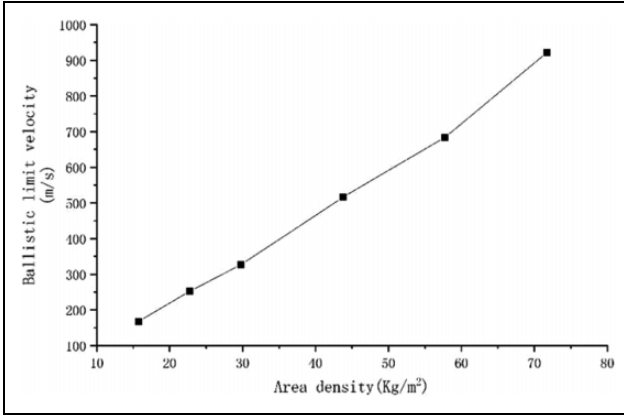
### Calculation of the ballistic limit velocity

The magnitude of the ballistic limit velocity of the fragment toward the target plate was an important indicator for measuring the penetrate effect of the fragment on the target plate and one of the main parameters for evaluating the power of the ammunition,<sup>20,21</sup> which was the average value of the highest velocity of the fragment partially penetrated the target plate and its minimum velocity when fully penetrated the target plate. The ballistic limit velocity of the fragment through the target plate could be characterized by  $v_{50}$ .<sup>22</sup> A large number of experiments had proved that  $v_{50}$  obeyed the normal distribution for a given target system. When the nonpenetration number was greater or less than the penetration number, the calculation formulas for  $v_{50}$  were as follows:

**Table 1.** Structure size and ballistic limit velocity of Ti/Al<sub>3</sub>Ti-laminated composites target.

No.	Thickness of the target plate (mm)	AD (kg/m <sup>2</sup> )	Ballistic limit velocity v <sub>50</sub> (m/s)	Energy absorption of the target (J)
1	4.5	15.75	168	114.31
2	6.5	22.75	252	257.19
3	8.5	29.75	327	433.06
4	12.5	43.75	516	1078.34
5	16.5	57.75	684	1894.82
6	20.5	71.75	922	3413.03

AD: area density; Ti/Al<sub>3</sub>Ti: titanium–titanium tri-aluminide.

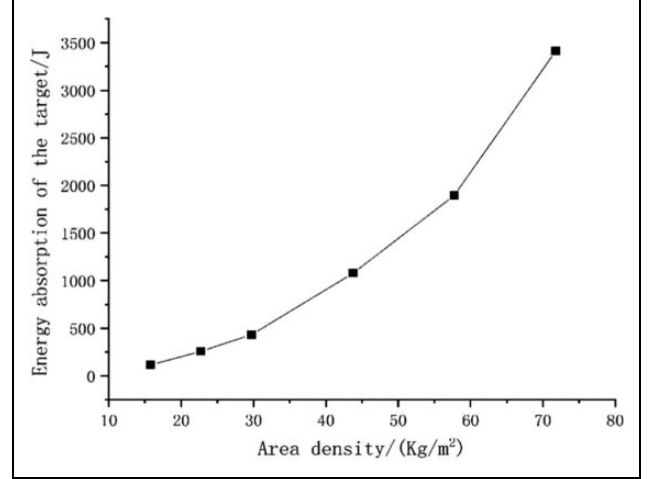
**Figure 2.** Ballistic limit velocity of Ti/Al<sub>3</sub>Ti-laminated composites target. Ti/Al<sub>3</sub>Ti: titanium–titanium tri-aluminide.

$$v_{50} = V_A + \frac{N_N - N_P}{N_N + N_P} (V_{N_{\max}} - V_A) \quad (1)$$

$$v_{50} = V_A + \frac{N_P - N_N}{N_N + N_P} (V_A - V_{P_{\min}}) \quad (2)$$

In the formula,  $V_A$  is the average value of all velocities in the mixed zone of penetration and nonpenetration,  $N_N$  is the number of the unpenetrated fragments in the mixed zone,  $N_P$  is the number of penetrating fragments,  $V_{N_{\max}}$  is the maximum velocity of the unpenetrated fragments,  $V_{P_{\min}}$  is the minimum velocity of the penetrated fragments.

Based on the above experimental scheme, using tungsten alloy spherical fragments for Ti/Al<sub>3</sub>Ti-laminated composite target plates with different surface densities, the ballistic performance experiments were performed at different impact velocities, and the corresponding ballistic limit velocities were obtained. The detailed parameters of the composite target plates are listed in Table 1, and Figure 2 shows the change law of the ballistic limit velocity with the target area density. It can be concluded that the energy absorption of the Ti/Al<sub>3</sub>Ti-laminated composite target varies with the target surface density near the ballistic limit velocity.

**Figure 3.** Energy absorption characteristics of Ti/Al<sub>3</sub>Ti-laminated composites target. Ti/Al<sub>3</sub>Ti: titanium–titanium tri-aluminide.

### Effect of the target area density on the ballistic energy absorption

Regarding tungsten balls as a rigid body, the energy absorption of penetrating the Ti/Al<sub>3</sub>Ti-laminated composite target could be calculated by the ballistic test results with the following formula:

$$E_a = \frac{1}{2} m_p v_i^2 - \frac{1}{2} m_p v_r^2 \quad (3)$$

In the formula,  $E_a$  is the energy absorbed by the target plate during the tungsten alloy spherical fragment penetrating the target plate,  $m_p$  is the mass of the tungsten alloy spherical fragment,  $v_i$  is the initial velocity before the tungsten alloy spherical fragment penetrating the target,  $v_r$  is the remaining velocity of the tungsten alloy spherical fragment that had penetrated the target plate.

At the ballistic limit velocity,  $v_r = 0$ , and  $E_a$  could be expressed as follows:

$$E_a = \frac{1}{2} m_p v_{50}^2 \quad (4)$$

The calculated result of the energy absorbed of the target is listed in Table 1, and Figure 3 shows the curve of the energy absorbed by the target as a function of its area density. It can be seen that the energy absorption of the Ti/Al<sub>3</sub>Ti-laminated composite target enhanced as the area density of the target increased near the ballistic limit velocity.

### The empirical formula for the ballistic limit velocity

The process of the tungsten alloy spherical fragment vertically penetrating the Ti/Al<sub>3</sub>Ti-laminated composite target was related to many parameters, and all of the thermal effects were ignored in this article. The main independent physical quantities that determined the ultimate ballistic velocity are summarized in Table 2.

It can be seen that the ballistic limit velocity of tungsten alloy spheres vertically penetrating a finite thickness of

**Table 2.** Independent physical quantities of controlling ballistic limit velocity.

Materials	Parameter name	Dimension
Tungsten alloy spherical fragment	Density $\rho_p$ ( $\text{kg}\cdot\text{m}^{-3}$ )	$\text{ML}^{-3}$
	Diameter $d_p$ (m)	L
	Sound velocity $C_p$ ( $\text{m}\cdot\text{s}^{-1}$ )	$\text{LT}^{-1}$
	Elasticity modulus $E_p$ (Pa)	$\text{L}^{-1}\text{MT}^{-2}$
	Shear modulus $G_p$ (Pa)	$\text{L}^{-1}\text{MT}^{-2}$
	Young's modulus $H_p$ (Pa)	$\text{L}^{-1}\text{MT}^{-2}$
	Yield strength $Y_p$ (Pa)	$\text{L}^{-1}\text{MT}^{-2}$
Ti/Al <sub>3</sub> Ti-laminated composite target	Density $\rho_t$ ( $\text{kg}\cdot\text{m}^{-3}$ )	$\text{ML}^{-3}$
	Thickness $h_t$ (m)	L
	Impact toughness $K_t$ (Pa)	$\text{L}^{-1}\text{MT}^{-2}$
	Elasticity modulus $E_t$ (Pa)	$\text{L}^{-1}\text{MT}^{-2}$
	Shear modulus $G_t$ (Pa)	$\text{L}^{-1}\text{MT}^{-2}$
	Hardening modulus $H_t$ (Pa)	$\text{L}^{-1}\text{MT}^{-2}$
	Yield strength $Y_t$ (Pa)	$\text{L}^{-1}\text{MT}^{-2}$
	Sound velocity $C_t$ ( $\text{m}\cdot\text{s}^{-1}$ )	$\text{LT}^{-1}$

Ti/Al<sub>3</sub>Ti: titanium–titanium tri-aluminide.

Ti/Al<sub>3</sub>Ti-laminated composite target was a function of 15 physical quantities, that is:

$$v = f(\rho_p, d_p, C_p, E_p, G_p, H_p, Y_p, \rho_t, h_t, C_t, K_t, E_t, G_t, H_t, Y_t) \quad (5)$$

Select  $\rho_p$ ,  $d_p$ , and  $Y_p$  as the independent dimensional physical quantities, and according to the principle of dimensional homogeneity, other derived quantities could be written as a dimensionless form as follows:

$$\begin{aligned} \Pi_1 &= \frac{C_p}{\sqrt{Y_p/\rho_p}}, \quad \Pi_2 = \frac{E_p}{Y_p}, \quad \Pi_3 = \frac{G_p}{Y_p}, \quad \Pi_4 = \frac{H_p}{Y_p}, \\ \Pi_5 &= \frac{\rho_t}{\rho_p}, \quad \Pi_6 = \frac{h_t}{d_p}, \quad \Pi_7 = \frac{C_t}{\sqrt{Y_p/\rho_p}}, \quad \Pi_8 = \frac{K_t}{Y_p}, \\ \Pi_9 &= \frac{E_t}{Y_p}, \quad \Pi_{10} = \frac{G_t}{Y_p}, \quad \Pi_{11} = \frac{H_t}{Y_p}, \quad \Pi_{12} = \frac{Y_t}{Y_p}, \\ \Pi &= \frac{v}{\sqrt{Y_p/\rho_p}} \end{aligned} \quad (6)$$

Based on the dimensional analysis  $\Pi$  theorem, the equation (3) was rewritten into a dimensionless parameter form as follows:

$$\Pi = \frac{v}{\sqrt{Y_p/\rho_p}} = f(\Pi_1, \Pi_2, \dots, \Pi_{12}) \quad (7)$$

The parameters of  $\Pi_1$  to  $\Pi_5$  and  $\Pi_7$  to  $\Pi_{12}$  were only related to the material properties. With the sphere and target plate materials determined, the above 11 similar parameters were satisfied by themselves. Therefore, equation (7) could be simplified as:

$$\Pi = \frac{v}{\sqrt{Y_p/\rho_p}} = f\left(\frac{h_t}{d_p}\right) \quad (8)$$

From the previous analysis, we could know that the ballistic limit velocity of tungsten alloy spherical fragments penetrating the Ti/Al<sub>3</sub>Ti-laminated composite target should follow the law of geometric similarity under the condition that the ball and target materials were unchanged. That is, the dimensionless ballistic limit velocity of the ball penetrating the target was only a function of the thickness of the target and the initial diameter of the ball.

Therefore, we could know from equation (7) that:

$$v = K \left(\frac{h_t}{d_p}\right)^\alpha \quad (9)$$

In the formula,  $K$  and  $\alpha$  are undetermined constants.

Taking the logarithm of both sides at the same time, we get the following equation:

$$\ln v = \ln K + \alpha \ln\left(\frac{h_t}{d_p}\right) \quad (10)$$

Assuming that,

$$y = \ln v, \quad A = \ln K, \quad x = \ln\left(\frac{h_t}{d_p}\right) \quad (11)$$

So,

$$y = A + \alpha x \quad (12)$$

Based on the results of ballistic experiments, multivariate linear regression was performed on equation (12), and the coefficients obtained from the regression were substituted into equation (9) to obtain the ballistic limit velocity of tungsten alloy spherical fragments vertically penetrating the Ti/Al<sub>3</sub>Ti-laminated composite target.

Therefore, the empirical relationship of the ballistic limit velocity of the tungsten alloy spherical fragment vertically penetrating the Ti/Al<sub>3</sub>Ti-laminated composite target was as follows:

$$v = 378 \left(\frac{h_t}{d_p}\right)^{1.12} \quad (13)$$

In the above formula,  $v$  is  $v_{50}$ . Since formula (13) was obtained based on the dimensional analysis and the fitting analysis was based on the experimental results, it was suitable for the tungsten alloy spherical fragment penetrating the Ti/Al<sub>3</sub>Ti-laminated composite target. The applicable parameter ranges were  $v < 950$  m/s and  $0.47 < h_t/d_p < 2.16$ .

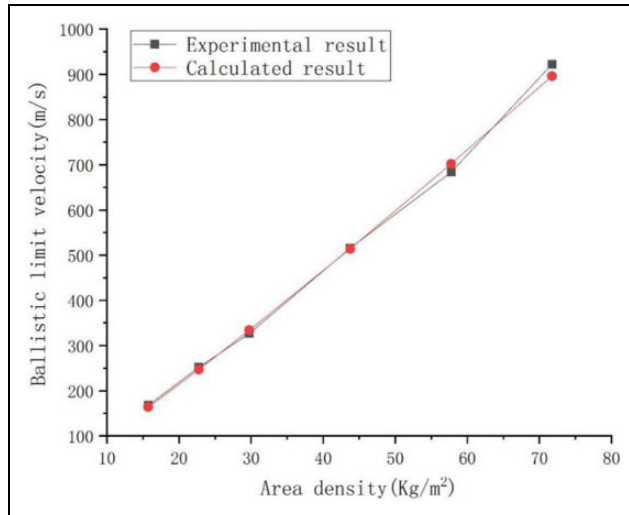


**Figure 4.** Comparison between experimental and calculated values of ballistic limit velocity.

**Table 3.** Comparison between experimental and calculated values of ballistic limit velocity.

No.	Ballistic limit velocity $v_{50}$ (m/s)		The relative error (%)
	Experimental result	Calculated values	
1	168	164	-2.4
2	252	247	-2
3	327	334	2.1
4	516	514	-0.4
5	684	702	2.6
6	922	896	2.4

Table 3 and Figure 4 present the comparison between the experimental value of the ballistic limit velocity of the tungsten alloy spherical fragment penetrating the Ti/Al<sub>3</sub>Ti-laminated composite target and the calculation result using formula (13).

From the data in Table 3 and Figure 4, it can be seen that for the tungsten alloy spherical fragment penetrating the Ti/Al<sub>3</sub>Ti-laminated composite target system, the average value of the relative error between the calculated value of the ballistic limit velocity and the experimental value was less than 2.7%, and the maximum single error was 3.8%, which met the requirements of engineering applications.

## Conclusions

1. The ballistic limit velocity of tungsten alloy spherical fragment and the ballistic energy absorbed by the target plate increased with a higher target area density of the Ti/Al<sub>3</sub>Ti-laminated composite.
2. The empirical relationship of the ballistic limit velocity of the tungsten alloy spherical fragment penetrating the Ti/Al<sub>3</sub>Ti-laminated composite target with different thickness was obtained by means

of the dimensional analysis method and the similar theory, and the calculation results coincided well with the experimental values and met the engineering calculation requirements.


## Declaration of conflicting interests


The author(s) declared no potential conflicts of interest with respect to the research, authorship, and/or publication of this article.

## Funding

The author(s) disclosed receipt of the following financial support for the research, authorship, and/or publication of this article: The work was financially supported by the National Natural Science Foundation of China (11802274) and open research fund of Key Laboratory of North University of China (Grant Nos. DXMBJJ2018-01).

## ORCID iD

Yingbin Liu  <https://orcid.org/0000-0002-4795-4173>

Meini Yuan  <https://orcid.org/0000-0002-9020-3789>

## References

1. Zhang Z-Y and Dai F. Applications of composite in the armored vehicles. *Plastics* 2000; 29: 38–42.
2. Cao Y, Zhu SF, Guo CH, et al. Numerical investigation of the ballistic performance of metal-intermetallic laminate composites. *Appl Compos Mat* 2015; 22: 437–456.
3. Peng LM, Li H and Wang JH. Processing and mechanical behavior of laminated titanium–titanium tri-aluminide (Ti–Al<sub>3</sub>Ti) composites. *Mat Sci Eng A* 2005; 406: 309–318.
4. Vecchio KS. Synthetic multifunctional metallic-intermetallic laminate composites. *JOM* 2005; 57: 25–31.
5. Li T, Jiang F, Olevsky EA, et al. Damage evolution in Ti6Al4V–Al<sub>3</sub>Ti metal-intermetallic laminate composites. *Mat Sci Eng A-Struct* 2007; 443: 1–15.
6. Li T, Al Olevsky E and Meyers MA. The development of residual stresses in Ti6Al4V–Al<sub>3</sub>Ti metal-intermetallic laminate (MIL) composites. *Mat Sci Eng A-Struct* 2008; 473: 49–57.
7. Price RD, Jiang F, Kulin RM, et al. Effects of ductile phase volume fraction on the mechanical properties of Ti–Al<sub>3</sub>Ti metal-intermetallic laminate (MIL) composites. *Mat Sci Eng A-Struct* 2011; 528: 3134–3146.
8. Galeev RM, Valiakhmetov OR, Safiullin RV, et al. Development of laminated composite materials based on orthorhombic aluminide/titanium alloy and their tensile mechanical properties. *Met Sci J* 2013; 25: 1485–1488.
9. Mirjalili M, Soltanieh M, Matsuura K, et al. On the kinetics of TiAl<sub>3</sub> intermetallic layer formation in the titanium and aluminum diffusion couple. *Intermetallics* 2013; 32: 297–302.
10. Yener T, Guler S, Siddique S, et al. Determination of the young modulus of Ti–TiAl<sub>3</sub> metallic intermetallic laminate composites by nano-indentation. *Acta Phys Pol A* 2016; 129: 604–606.

11. Zhou PJ, Guo CH, Wang EH, et al. Interface tensile and fracture behavior of the Ti/Al<sub>3</sub>Ti metal-intermetallic laminate (MIL) composite under quasi-static and high strain rates. *Mat Sci Eng A-Struct* 2016; 665: 66–75.
12. Lin C, Han Y, Guo C, et al. Synthesis and mechanical properties of novel Ti-(SiCf/Al<sub>3</sub>Ti) ceramic-fiber-reinforced metal-intermetallic-laminated (CFR-MIL) composites. *J Alloys Compd* 2017; 722: 427–437.
13. Lazurenko DV, Bataev IA, Mali VI, et al. Synthesis of metal-intermetallic laminate (MIL) composites with modified Al<sub>3</sub>Ti structure and in situ synchrotron X-ray diffraction analysis of sintering process. *Mat Des* 2018; 151: 8–16.
14. Liu J, Zhang L, Jiang F, et al. Elasto-plastic mechanical properties and failure mechanism of innovative Ti-(SiCf/Al<sub>3</sub>Ti) laminated composites for sphere-plane contact at the early stage of penetration process. *Materials* 2018; 11: 1152.
15. Yuan MN, Li L and Wang ZJ. Study of the microstructure modulation and phase formation of TiAl<sub>3</sub>Ti laminated composites. *Vacuum* 2018; 157: 481–486.
16. Zelepugin SA and Zelepugin AS. *Numerical simulation of multilayer composites failure under dynamic loading*. In: *Applied Mechanics and Materials 2015* (Vol. 756, pp. 408–413). Trans Tech Publications, 2015.
17. Li T, Grignon F, Benson D, et al. Modeling the elastic properties and damage evolution in Ti–Al<sub>3</sub>Ti metal–intermetallic laminate (MIL) composites. *Mat Sci Eng A* 2004; 374: 10–26.
18. Grujicic M, Snipes JS and Ramaswami S. Penetration resistance and ballistic-impact behavior of Ti/TiAl<sub>3</sub> metal/intermetallic laminated composites (MILCs): a computational investigation. *AIMS Mater Sci* 2016; 3: 10.3934.
19. Cao Y, Zhang D, Liu J, et al. Modeling for impact damage and failure analysis of Ti/Al<sub>3</sub>Ti laminate composite. *Mater Sci Eng C* 2019; 42: 116–121.
20. Xu Y, Wang S and Bo X. Armor-piercing ultimate of tungsten alloy spherical fragment against low-carbon steel. *J Vib Shock* 2011; 30: 192–195.
21. Mao L, Wang H, Jiang C-L, et al. Ballistic limit velocity of tungsten alloy spherical fragment penetrating ceramic/DFRP composite target plates. *J Vib Shock* 2015; 34: 1–4.
22. Li J (transl.). *Design for terminal effects*. Beijing: National Defense Industry Press, 1988.